Microgrid Composed of Three or More SOFC Combined Cycles without Accumulation of Electricity

Shin'ya Obara
Kitami Institute of Technology, Power Engineering Lab., Dep. of Electrical and Electronic Engineering
Koen-cho 165, Kitami, Hokkaido 090-8507, Japan
obara@mail.kitami-it.ac.jp
phone/FAX +81-157-26-9262

Jorge Morel
Kitami Institute of Technology, Power Engineering Lab., Dep. of Electrical and Electronic Engineering
Koen-cho 165, Kitami, Hokkaido 090-8507, Japan

Abstract

Large-scale centralization of the power supply system, consisting mainly of nuclear power generation and thermal power generation, has been adopted in Japanese electrical power system. Because Japan's centralized power supply system has little accommodation for changes in load, the amount of renewable energy that can be introduced is restricted substantially. The percentage of renewable energy introduced in Japan in 2012 was 1.6%; if this were to include hydraulic power generation, the percentage would be less than 10%. Accordingly, this study develops a microgrid that responds to the changes in output from a large-scale solar power system by using load from the operation of three or more solid oxide fuel cell hybrid power systems (PGSSs), and controlling the number of PGSS units in response to the magnitude of load. A storage battery is not used for the microgrid developed in this paper for control of the change in output from renewable energy, the proposal of a system with an introductory high rate of renewable energy is the purpose of this study. The study clarified the method of system operation and the rate at which renewable energy can be introduced at the time of developed microgrid distributed installation, using three or more PGSSs to supply all the cities in the Hokkaido region of Japan. From the results of the analysis, the control achieved with the PGSS units was confirmed to be effective. Furthermore, according to meteorological data and our proposed microgrid, the power supplied by renewable energy over the entire Hokkaido region in 2012 reached 48% on February 14 (winter), 49% on July 15 (summer), and 45% on October 15 (moderate season).

Key Words: Microgrid, SOFC combined cycle, Photovoltaics, Mega-solar power plant, Number control

1. Introduction

The main electrical power systems in Japan are composed of a centralized power supply system that uses nuclear, thermal, and hydraulic power generation. However, Japan's centralized power supply system consists of nine areas, each of which uses the power composition considered economically optimal in that area [1-3]. Although accommodating electrical demands between areas is possible, restriction of the electrical traffic and the differences in frequency between areas are subjects for improvement; currently there are few accommodations for electric energy. So far, electric power quality of the Japanese electrical power system has remained dramatically stable, and within the country it is thought that the system has world class technology. On the other hand, the serious problems faced by the Japanese centralized power supply system became clear after the accident caused by the tsunami at the first Fukushima nuclear power station in March 2011. Safety is checked at all nuclear power stations in Japan, and trials to increase the amount of power interchange between areas have been conducted. Furthermore, increases in the amount of renewable energy introduced and the supply of stable power from the distributed power supply are also under investigation. The percentage of renewable energy introduced in Japan in 2012 was 1.6%; if this were to include hydraulic power generation, the percentage would increase to approximately 10%. To promote greater increases in the use of renewable energy, as well as to stabilize the power supply, large-scale batteries and pumped hydropower generation must be introduced into the electrical power system [4, 5]. However, it is difficult to realize the introduction of a large-scale battery because of the drastic increase in cost that would accrue, and the use of pumped hydropower generation is deemed impractical. Therefore, to increase the rate at which renewable energy is introduced into the electrical power system for the purpose of this study, a microgrid from a power generation system (PGS) that uses a solid oxide fuel cell (SOFC)-combined cycle (SCC), i.e., a PGS SCC (hereafter, PGSS) [6-10], which can accommodate changes in output from renewable energy was checked an effect by a numerical analysis.

The maximum power-generation efficiency of the PGSS exceeds 50%, since the PGSS has a gas turbine and a steam turbine, it is expected that partial load operation with the output change of renewable energy is possible for the output of a gas turbine and a steam turbine. Moreover, load changes for short periods in a microgrid are stabilized by the inertial force of each turbine. Furthermore, the highly efficient and stabilized electrical power system (microgrid) by a battery is developed by controlling the number of PGSSs in operation in response to the magnitude of the load.

Currently, Hokkaido Electric Power Co., Inc. supplies electric power to all areas of Hokkaido in Japan by use of nuclear power generation, thermal power generation, hydraulic power generation, and alternative energy, which generate 2.07 GW (three sets), 4.21 GW (in 12 places including those planned), 1.24 GW (in 53 places including those under construction), and 0.026 GW (in two places), respectively. Hokkaido is divided into seven areas, with the existing hydroelectric power station considered for this study, with each area having a suitable type of SCC. Moreover, this study aims at increasing the renewable energy rate of the entire Hokkaido

region to approximately 50% by installing a mega-scale solar power plant (MSP) in the microgrid of each area. Three or more PGSSs are installed in a microgrid, and the output of the PGSSs is adjusted in response to MSP fluctuations. The purpose of this study is to clarify (1) the method of operating a PGSS and (2) the power supply rate using renewable energy in each microgrid composed of PGSSs and renewable energy (MSPs and hydraulic power generation), and the system whose introductory rate of renewable energy is very large is built. Furthermore, basic data on an electrical power system using a distributed power supply is obtained by investigating the load factor of the PGSS, the net thermal efficiency, and the characteristics of operating time in each developed microgrid.

2. Electrical Power System of Hokkaido

Hokkaido has a population of about 5.5 million (2010), which is approximately 4.3% of Japan's population. It comprises an area of 83,450 km^2, and the whole region has mostly a subarctic zone humid climate. Temperature varies greatly between summer and winter, with heavy snowfall and severe cold in the northern and eastern parts. Average temperature during the coldest month over the entire Hokkaido region (except along the coast) is below −8 °C. The inland outside air temperature reaches below −30 °C. Figure 1 shows a map of the arrangement of power sources and the 2013 capacity of Hokkaido Electric Power Co., Inc (the official announcement data of the Hokkaido Electric Power Co., Inc.). The broken line in the figure denotes equipment under plan. All power sources are interconnected by the power grid, and electric power generated by a large-scale nuclear power station and a thermal power plant is supplied to all areas of Hokkaido. Moreover, Hokkaido's energy demand peaks in February because of winter heating load. Although traditional heating systems in Hokkaido generally utilize kerosene space heating, the use of electric air-source heat pumps is expected to increase.

Figure 2 shows the case of the operation record of Hokkaido Electric Power Co., Inc. on a representative day in December 2010 (the official announcement data of the Hokkaido Electric Power Co., Inc.). Because the power-source scheme of Hokkaido Electric Power has a large percentage of nuclear power generation and a thermal power generation system (Fig. 2), neither of which allows changes in output, changes in the output of renewable energy cannot be absorbed. Furthermore, although Tomari nuclear power station, Sapporo, Tomakomai, and Muroran are connected with the large-capacity power grid, power transmission lines with very small capacity are installed in other areas with much potential for renewable energy. To avoid the influence of fluctuations in renewable energy, Hokkaido Electric Power has stopped accepting new renewable energy. When the equipment under plan is included, about 0.37 MW of renewable energy is planned in Hokkaido.

In this study the power-source scheme shown in Figs. 1 and 2 is newly replaced with distribution from a microgrid composed of PGSSs and renewable energy (from the MSPs and the hydroelectric power station).

Because a gas turbine and a steam turbine are installed in the PGSS, load changes of short duration are absorbable by the microgrid, depending on the inertial force of each turbine. Furthermore, it is through that efficient power generation can be attained even under large changes in the output of renewable energy by introducing a control on the number of PGSS units, corresponding to the magnitude of load, all without using a battery. The proposed system can successfully introduce a substantial amount of renewable energy by implementing the technology improvements described above. The study aims at supplying the electric power of half of all power sources by use of renewable energy. The 35 cities are located in Hokkaido are divided into seven areas with the proposed microgrid introduced into each area. Because each microgrid is interconnected with power transmission lines and the local supply and local consumption of energy are introduced in each microgrid, the capacity of the power transmission lines for interconnection is very small.

3. Power Generation System with SOFC Combined Cycle (PGSS)

3.1 Configuration of the PGSS

Figure 3 shows the configuration of the PGSS assumed in this study (proposed system). Figure 3 (a) shows the tri-generation system (System A), consisting of a SOFC, a gas turbine, and a steam turbine, which uses natural gas as the fuel. Moreover, Fig. 3 (b) shows the SOFC combined cycle [i.e., the integrated gasification fuel cell (IGFC) power generation (System B)] with a coal gasification furnace. There are many coal mines in Hokkaido, so IGFC has been introduced in areas near coal mining regions. The gas turbine and steam turbine of the PGSS shown in Fig. 3 are operated with a number of constant rotations, and electric power of 50 Hz three-phase-circuit alternating current is supplied to the power grid. The voltage at the generating end is adjusted in the range 100–275 kV by each microgrid, because the conditions at the demand side differ. Moreover, when a PSGG is installed near an urban area, the exhaust heat from Systems A and B can be used to supply hot water and space heating; however, this study assumed that all corresponding heat loads are based on the use of electric air-source heat pumps.

3.2 Efficiency of PGSS

Figure 4 shows the net thermal efficiency of the SOFC and the PGSS [11] (the official announcement data of the Mitsubishi Heavy Industries Co., Inc.): net thermal efficiency of the SOFC tri-generation system (System A) is the highest, with IGFC (System B) coming in next. Net thermal efficiency of each system is dependent on the load factor of the system, with the minimum load of each system set at 40%. Figure 5 shows the relation between capacity and thermal efficiency in a gas turbine/steam turbine combined cycle [12] (the official announcement data of the GE Power Systems). Because thermal efficiency increases as the capacity of the system increases, it is necessary to change the characteristics of net thermal efficiency in accordance

with the rated capacity of the system. The relation between capacity and thermal efficiency shown in Fig. 5 is used for the calculation of net thermal efficiency for each system in this study.

3.3 System Configuration of Microgrid

Figure 6 shows the system configuration of the microgrid taken into consideration by this study installed in each area. Three or more PGSSs, wind turbines, a photovoltaic system (mega-solar power plant, MSP), and hydraulic power generators as shown in Fig. 6 can be installed in areas A–G. The hydraulic power generator uses the present facilities and capacity, and the number of PGSSs installed and the MSP are determined from the power load and the amount of solar radiation in each area, as described in Section 4. If two or more changeable-output components (e.g., wind turbines and MSP) are factored into the control of the number of PGSS units, the analysis of output will become complicated. Accordingly, the decision to install an MSP and/or one or more hydraulic power generators was made in this study because renewable energy is introduced into the proposed microgrid. Moreover, the proposed microgrid is not accompanied by a storage battery, which substantially reduced the facilities cost of the microgrid.

Capacity of the equipment constituting each microgrid is determined from the magnitude of electricity demand in that particular area. Although the microgrids of each area are interconnected by power transmission lines, electric energy transfer between the microgrids for the purpose of accommodation is fundamentally zero. Therefore, the interconnection between microgrids is not taken into consideration in this research. Beyond the scope of this research, interconnection of the microgrid is necessary to

a. transport surplus renewable energy to other areas,
b. control electricity fluctuations in a transmission network by use of renewable energy in the whole region, and
c. accommodate the delivery of electric power in an emergency.

4. Layout of the Microgrid

4.1 Definition of Area

The 35 cities in Hokkaido are divided into seven areas, A–G, as shown in Fig. 7, and the type of PGSS installed in each area is indicated in the figure. Figure 7 shows the original scheme of this study. Systems A and B from Fig. 3 differ in fuel, using natural gas and coal, respectively. Areas E, F, and G are coal mining regions, so System B is used there, with System A used in the other areas.

4.2 Power Load Patterns

4.2.1 Power Load

Figure 8 shows the monthly record of mean power supplied by Hokkaido Electric Power Co., Inc. in 2010 (the official announcement data of the Hokkaido Electric Power Co., Inc.). The maximum load appears in winter (February), and the minimum load appears in the moderate seasons (May and October). Therefore, the following section investigates PGSS operation on representative days in winter (February), a moderate season (October), and summer (July). Figure 9 (the official announcement data of the Hokkaido Electric Power Co., Inc.) shows the characteristic distribution of electricity demand for areas A–G on a representative day in December 2010 (compare this figure to Figure 2, the pattern of power generation in the entire Hokkaido region for the same day).

4.2.2 Power Consumption of Heat Pump

The coefficient of performance (COP) for an electric air-source heat pump changes with outside air temperature. The COPs shown in Fig. 10 were used to calculate the power consumption of the heat pump [13] (the official announcement data of the Mitsubishi Heavy Industries Co., Inc.). The COP of the heat pump at each hour on a representative day was calculated by introducing outside air temperatures measured for each area into Fig. 10. Furthermore, power load of the heat pump was calculated by dividing heat load calculated from the population and number of households of each area by the COP obtained from Fig. 10. Sum total of the power load on the representative day in each area is shown in Fig. 8, and power load of the heat pump, in Fig. 11. Total electricity supplied to the microgrid by the PGSSs, MSP, and hydraulic power generators in each area corresponds to the power load pattern shown in Fig. 11.

4.3 Operating Conditions for the PGSS

The rated output of the PGSS is set to the same value for all the microgrids in areas A–G. To improve efficiency at times of partial load, the numbers of PGSS units have been controlled, with at least three sets of PGSSs introduced into each microgrid. The rated output of one PGSS set introduced into the microgrid of area i (i = 1, 2, ..., the total number of areas) is set to $Q_{c,i}$, the power load at time t is set to $q_{p,i,t}$, and the electric-power output of the MSP is set to $q_{pv,i,t}$. In this case, the number of PGSSs in operation at 100% of load factor is a value from the integer part of Eq. (1). On the other hand, the value below the decimal point of $n_{d,i,t}$ is load outputted by one PGSS set with a load factor of less than 100% (partial load).

$$n_{d,i,t} = \frac{q_{p,i,t} - q_{pv,i,t}}{Q_{c,i}} \tag{1}$$

The conditions that control the number of PGSS units and the conditions of load factor are as follows.

a. The value of the integer part of $n_{d,i,t}$ obtained by Eq. (1) is the number of PGSSs operating at full load.

b. The value below the decimal point of $n_{d,i,t}$ obtained by Eq. (1) is the value for one PGSS set operating at partial load. However, the minimum load factor of all the PGSSs is set to 40%; even when

the load factor is less than 40% from the calculation results below the decimal point in Eq. (1), the load factor for the PGSS is compulsorily 40%.

c. The rated output $Q_{c,i}$ of a PGSS in Eq. (1) is the annual maximum power load in area i and the sum total of reserve capacity (10% of the maximum dissipation load).

4.4 Amount of Renewable Energy Introduced

4.4.1 Potential Quantity of Renewable Energy

Figure 12 shows monthly average data on amount of global solar radiation and wind speed around the cities included in each area [14, 15] (Publication data of Japan Meteorological Agency). Although the global solar radiation and wind speed vary in each area, the annual relative trend is almost the same. Accordingly, as shown in Fig. 12, the amount of global solar radiation is large from spring to summer, and small in winter. In contrast, the wind speed is fast in winter and slow in summer. Therefore, although the quantity of renewable energy in each area of Hokkaido shown in Fig. 7 varies, the tendency by season is common to all the areas. Since global solar radiation and wind speed reverse their tendencies in summer and winter, if suitable amounts of both are introduced, the supply of renewable energy will be stable throughout the year.

4.4.2 Array Area of the MSP

When the output from renewable energy exceeds the quantity demanded by the microgrid in one area, operating the PGSS in that area will become unnecessary. However, to prepare for quick rises in PGSS output, even if the output from renewable energy exceeds the amount demanded, this study always operates one PGSS set at 40% of minimum load. If the maximum load $q_{p,i,\max}$ for one year in the area i microgrid and the amount of insolation $q_{r,i,i}$ (for the south, inclination angles are 40°) in the representative city included in area i [14] are both entered into Eq. (2), the area $S_{msp,i}$ of the MSP solar cell array installed in area i can be obtained, where $Q_{c,i}$ is the rated output of the PGSS, η_{msp} is the conversion efficiency of photovoltaics, η_{msp} is 18%, and $q_{r,i,i}$ uses the average value of observational data for the past ten years (see the analysis given in the next section). Moreover, the difference in the conversion efficiency created by the temperature change in the solar cell array is not taken into consideration.

$$S_{msp,i} = \frac{q_{p,i,\max} - 0.4 \cdot Q_{c,i}}{\eta_{msp} \cdot q_{r,i,i}} \tag{2}$$

Table 1 shows the maximum power load for each area, capacity, number of PGSSs installed, array area and set position of the MSP, and rated output of hydroelectric power stations. Since many large and/or industrial cities are included in area A, electricity demand there is dramatically larger than in other areas. Consequently, 10 sets of 1.0 GW PGSSs are installed in area A. Although the MSP array area would also be expected to be very large in area A, a wind farm and an MSP are installed in the same area, so the MSP array area has been reduced after taking into account the capacity introduced by the wind farm.

5. Analysis Procedure

The procedure for analyzing the number of PGSSs in operation and their load factors by controlling the number of PGSS units at area i and time t is outlined here.

a. Use Figs. 4 and 5 to determine the relation between PGSS load factor and net thermal efficiency and between PGSS capacity and thermal efficiency, respectively.
b. Apply Fig. 7 to the arrangement of the microgrids.
c. Prepare population, number of households, past meteorological data (outside air temperature and amount of insolation), and data on power load $q_{el,i,t}$ and heat load $q_{h,i,t}$ of area i (i = 1,2,..., the total number of areas). Use the observational data on February 14, July 15, and October 15, 2012, as the meteorological data for analysis.
d. Calculate the power load $q_{hp,i,t}$ consumed by the heat pump from the relation between outside air temperature and COP shown in Fig. 10, and between outside air temperature data and thermal load data.
e. By adding the power load $q_{hp,i,t}$ of the heat pump and the power load $q_{el,i,t}$ from step c (already obtained), obtain the power load $q_{p,i,t}$ at time t on a representative day of every month in area i (Fig. 11) as shown in Eq. (3).

$$q_{p,i,t} = q_{el,i,t} + q_{hp,i,t} = q_{el,i,t} + q_{h,i,t} / c_{hp,i,t} \quad (3)$$

where $c_{hp,i,t}$ is the COP of the heat pump.

f. Obtain the area $S_{msp,i}$ of the MSP solar cell array installed in area i from Eq. (2) in Section 4.4.2. Furthermore, obtain the electricity produced by the MSP $q_{pv,i,t}$ by multiplying $S_{msp,i}$ (described above) by $q_{r,i,i}$, and use the conversion efficiency η_{msp}.
g. Obtain the production of electricity $q_{scc,i,t}$ required of the PGSS from the power balances [Eq. (4)]. Furthermore, determine the number of PGSSs in operation in area i and the load factor for every PGSS by calculating Eq. (1) in Section 4.3.
h. After completing steps a–g above, determine the rate at which renewable energy can be introduced into an area by calculating the power supplied to the microgrid by the PGSSs, the MSP, and hydraulic power generators.

$$q_{scc,i,t} + q_{pv,i,t} = q_{p,i,t} \quad (4)$$

6. Analysis Results

6.1 Method of PGSS Operation

Figures 13 to 19 show the analysis results of the net thermal efficiency of each PGSS in areas A–G when (a) not installing the MSP and (b) the MSP is first installed. The net thermal efficiency of PGSSs 1 and 2 in Fig. 13 (a) maintains high values on the representative day of every month. The net thermal efficiency shows such high values that the PGSS load factor is as large as that in Fig. 4. On the other hand, since the load factor is small, the time zones with low net thermal efficiency appear in PGSS 3 of Fig. 13 (a); PGSSs 4–10 suspended operation on representative days in July with little heat load. Only PGSS 9 operated at 6:00 a.m. on the February day, accompanied by a large heat load.

Since 10% of the maximum load is designed as being the PGSS reserve capacity, PGSS 10 in Fig. 13 (a) was never operated. Furthermore, since the minimum load of the PGSS is fixed at 40% when the load is small (except for zero load), drops in net thermal efficiency are controlled by partial load operation. Although the amount of power consumed by the heat pump is large, PGSSs 6–9 in Fig. 13 (a) experience limited operation in February. Therefore, if the electric power consumption of the heat equipment is reducible, substantially fewer PGSSs will be installed.

6.2 Influence of MSP

Figure 13 (b) shows the analysis results for the net thermal efficiency of the PGSS when the MSP was first introduced into area A. The electric power from the MSP is outputted in the daytime, and PGSSs 1–3 in Fig. 13 (b) do not operate in that time zone during daytime. PGSSs 8 to 10 do not operate for an entire year. After the MSP is introduced, all hours of PGSS operation are less than that in Fig. 13 (a). The tendencies exhibited by PGSS load factor, net thermal efficiency, and hours of operation after the introduction of the MSP are also common in other areas, according to the analysis results (Figs. 14 to 19).

The analysis results for net thermal efficiency in each area are shown in Table 2. The output characteristics of the MSP act to reduce the load factor of the PGSSs, and the MSP installed in each microgrid causes a drop in the net thermal efficiency. Moreover, the net thermal efficiency in area A is the highest shown in Table 2. Because System A, with high power generation efficiency, is introduced in area A, more PGSSs are installed in area A than in other areas, so drops in efficiency at times of partial load are improved by precise control of all the units.

6.3 Rate at Which Renewable Energy Is Introduced

Figure 20 shows the analysis results of the supply rate of renewable energy (MSP and hydroelectric power station) on the representative day of every month in each area. The reason the supply rates of renewable energy vary in each area is because the regional differences in the amounts of insolation were large on February 14, July 15, and October 15 in 2012. On the other hand, Fig. 21 shows the analysis results of the supply of electric power generated by renewable energy compared to the annual power supplied in all areas. The electric power

296 percentages supplied by renewable energy for the entire Hokkaido area were 48%, 49%, and 45% when
297 introducing the proposed microgrid in February (winter), July (summer), and October (moderate season),
298 respectively.
299
300 6.4 Hours of PGSS Operation in Each Area
301 Figure 22 shows the analysis results of investigating the operation of the MSP in each microgrid. Results
302 for the microgrid without the MSP reached 100% for some areas in some months. Figure 22 (a) shows the
303 analysis results of the average load percentages for all PGSSs for every area, Figure 22 (b) shows the average
304 net thermal efficiency, and Fig. 22 (c) shows the hours of operation for all PGSSs. In calculating the average
305 load percentage and the average net thermal efficiency, PGSSs with zero output were under warm-up. PGSSs
306 were operated frequently with partial loads; if an MSP was introduced into a microgrid as shown in Figs. 22
307 (a) and (b), the average net thermal efficiency fell in almost all cases, unlike the response of a microgrid
308 without an MSP. However, as an effect of controlling the number of PGSS units, the hours of PGSS operation
309 in each area decreased greatly as shown in Fig 22 (c). As a result, the fuel quantity supplied to the PGSS in
310 the microgrid can be reduced greatly, as can the capacity and the number of PGSSs installed. However, since
311 the MSP output changes sharply according to the weather, reducing the PGSS capacity and the installed
312 number is restrictive. Moreover, if electric power transfer between microgrids is accommodated and the
313 introduction of wind farms is considered in future studies, it is expected that the number of PGSSs installed
314 will decrease further.
315
316 **7. Conclusions**
317 Changes in output from renewable energy (i.e., changing loads) can be accommodated in a microgrid
318 consisting of a PGS that uses a PGSS. Even without the use of a storage battery, high percentages of renewable
319 energy are expected to be utilized. By arranging microgrids in the Hokkaido region of Japan to control the
320 number of PGSS units on-line, and by installing an MSP and hydraulic power generation (sources of renewable
321 energy) in the microgrids, methods were investigated for operating the microgrids in a manner that increases
322 the percentage of renewable energy used. As a result, the following conclusions were obtained.
323 (1) If the number of PGSSs in operation is controlled in response to the magnitude of the microgrid load, the
324 total hours of PGSS operation will decrease greatly. Although maximum efficiency falls when the number of
325 PGSS units in the microgrid is controlled, owing to the decline in capacity of each PGSS, the net thermal
326 efficiency of the whole microgrid increases.
327 (2) The output of the MSP acts to reduce the load factor of the PGSSs, which lowers the net thermal efficiency.

(3) If the power consumption of heat pumps is large (e.g., winter), the PGSSs will operate for a greater number of hours. On the other hand, if the electric power consumption of heat equipment is reducible, the number of PGSSs installed in the microgrid can be reduced substantially.

(4) In the proposed system, the percentages of electric power supplied from renewable energy in the entire Hokkaido region using meteorological data from February 14, July 15, and October 15, 2012, were 48%, 49%, and 45% in February (winter), July (summer), and October (moderate season), respectively.

Highlights

Clarified a method for operating a microgrid consisting of a SOFC hybrid power system

Net thermal efficiency and total operating time by control of SOFC hybrid power units

Clarified percentage of microgrid power supplied by renewable energy

References

[1] Hayashi M, Hughes L, The policy responses to the Fukushima nuclear accident and their effect on Japanese energy security. Energy Policy 2013;59:86-101.

[2] Hondo H, Life cycle GHG emission analysis of power generation systems: Japanese case. Energy 2005;30:11:2042-2056.

[3] Valentine S, Sovacool B, The socio-political economy of nuclear power development in Japan and South Korea. Energy Policy 2010;38:12:7971-7979.

[4] Poullikkas A, A comparative overview of large-scale battery systems for electricity storage. Renewable and Sustainable Energy Reviews 2013;27:778-788.

[5] Daud M, Mohamed A, Hannan M, An improved control method of battery energy storage system for hourly dispatch of photovoltaic power sources. Energy Conversion and Management 2013;73:256-270.

[6] El-Emam S. R, Dincer I, Naterer F. G., Energy and exergy analyses of an integrated SOFC and coal gasification system. International Journal of Hydrogen Energy2012;37:1689-1697.

[7] Barelli L, Bidini G, Ottaviano A, Part load operation of SOFC/GT hybrid systems: Stationary analysis. International Journal of Hydrogen Energy, 2012:37;16140-16150.

[8] Musa A, Paepe D M, Performance of combined internally reformed intermediate/high temperature SOFC cycle compared to internally reformed two-staged intermediate temperature SOFC cycle. International Journal of Hydrogen Energy 2008;33:4665-4672.

[9] Barelli L, Bidini G, Gallorini F, Ottaviano A, An energetic–exergetic comparison between PEMFC and SOFC-based micro-CHP systems. International Journal of Hydrogen Energy 2011;36:3206-3214.

[10] Yan Z, Zhao P, Wang J, Dai Y,Thermodynamic analysis of an SOFC–GT–ORC integrated power system with liquefied natural gas as heat sink. International Journal of Hydrogen Energy 2013;38:3352-3363.

362 [11] Kobayashi Y, et al., Extremely high efficiency power system –SOFC triple combined cycle system.
363 Mitsubishi Heavy Industries Technical Review 2011;48:3:16-21. In Japanese.
364 [12] Chase D, Kehoe P, GE Combined Cycle Product Line and Performance. GE Power Systems 2011; GER-
365 3574g:1-40.
366 [13] Mitsubishi Heavy Industries, LTD., The Development of the CO2 Heat Pump Hot Water Supply Unit for
367 Business Use that can be Operated Down to -25 Degrees Celsius of Outside Air Temperature. Mitsubishi
368 Heavy Industries Technical Review 2011;48:4:86-88. In Japanese
369 [14] Annual amount-of-insolation data base (METPV-11), New Energy and Industrial Technology
370 Development Organization (NEDO), http://www.nedo.go.jp/library/nissharyou.html ;2013.
371 [15] The past meteorological data, Information of the climatological statistics, Japan Meteorological Agency,
372 http://www.data.jma.go.jp/obd/stats/etrn/ ;2013.
373

Captions

Fig. 1. Major sources of power generation for Hokkaido Electric Power Co., Inc.

Fig. 2. Composition of the electric power supply of Hokkaido Electric Power Co. Inc. on a representative day in December 2010.

Fig. 3. SOFC combined cycle; (a) SOFC tri-generation cycle (System A), (b) IGFC (System B).

Fig. 4. Partial load performance of each system.

Fig. 5. Relationship of thermal efficiency and net plant power for the gas turbine/steam turbine combined cycle (General Electric, 2011).

Fig. 6. Proposed energy distribution system.

Fig. 7. Planned arrangement for the energy system in Hokkaido.

Fig. 8. Monthly averages of the daily variation in the electric power supply produced by Hokkaido Electric Power Co., Inc. in 2010 (a) from January to June and (b) from August to December.

Fig. 9. Electric power supplied by each area on a representative day in December 2010.

Fig. 10. Heat pump performance.

Fig. 11. Electric power supplied by Hokkaido Electric Power Co., Inc. on a representative day in December 2010.

Fig. 12. Monthly amount of insolation and the wind speed in each area.

Fig. 13. Analysis results of the net thermal efficiency of area A using (a) System A without MSP and (b) System A with MSP.

Fig. 14. Analysis results of the net thermal efficiency of area B using (a) System A without MSP and (b) System A with MSP.

Fig. 15. Analysis results of the net thermal efficiency of area C using (a) System A without MSP and (b) System A with MSP .

Fig. 16. Analysis results of the net thermal efficiency of area D using (a) System A without MSP and (b) System A with MSP.

399 Fig. 17. Analysis results of the net thermal efficiency of area E using (a) System B without MSP and (b)
400 System B with MSP.

401 Fig. 18. Analysis results of the net thermal efficiency of area F using (a) System B without MSP and (b)
402 System B with MSP.

403 Fig. 19. Analysis results of the net thermal efficiency of area G using (a) System B without MSP and (b)
404 System B with MSP.

405 Fig. 20. Analysis results of the rate of renewable energy for each area in February, July, and October 2012.

406 Fig. 21. Percentage of renewable energy in comparison to total energy supplied.

407 Fig. 22. Analysis results of the influence of introducing MSP; (a) average load factor, (b) average net thermal
408 efficiency, and (c) average total operating time of the system.

409 Table 1. Number of installed PGSSs.

410 Table 2. Net thermal efficiency of areas A–G.

411
412
413

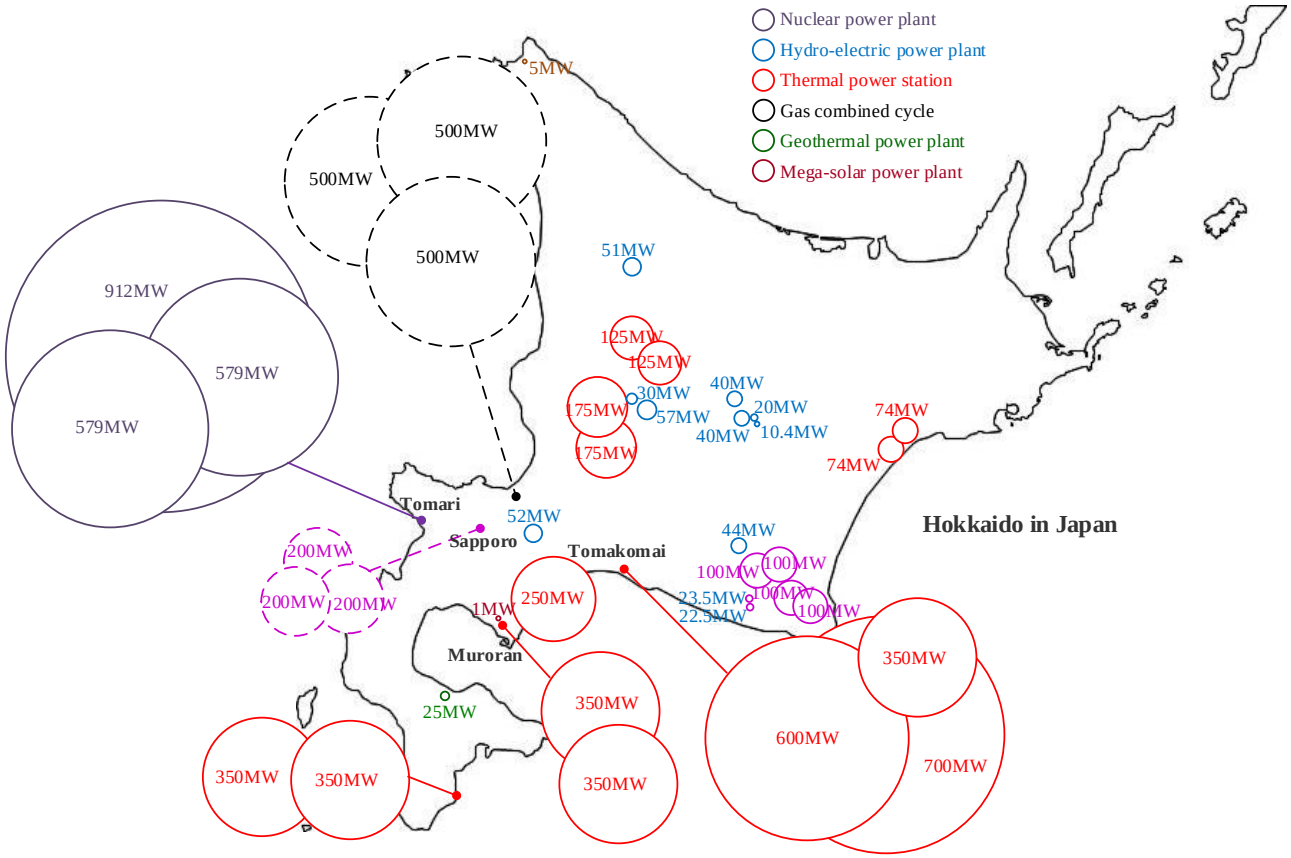

414

415 Fig. 1

416

417

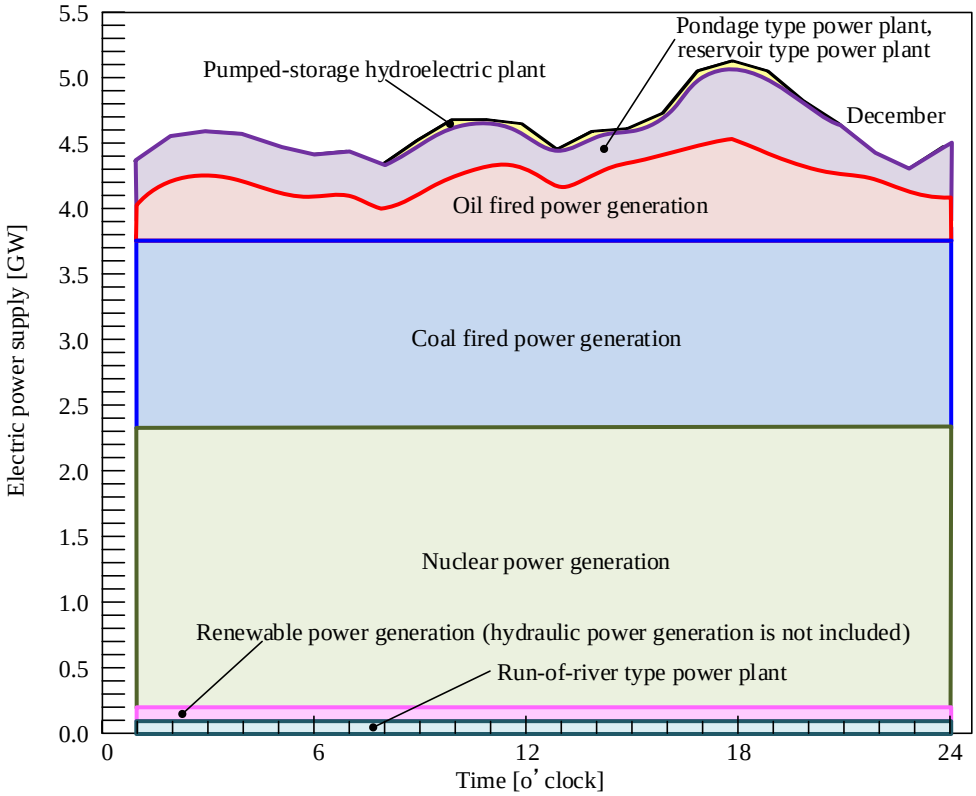

418

419 Fig. 2

420

421

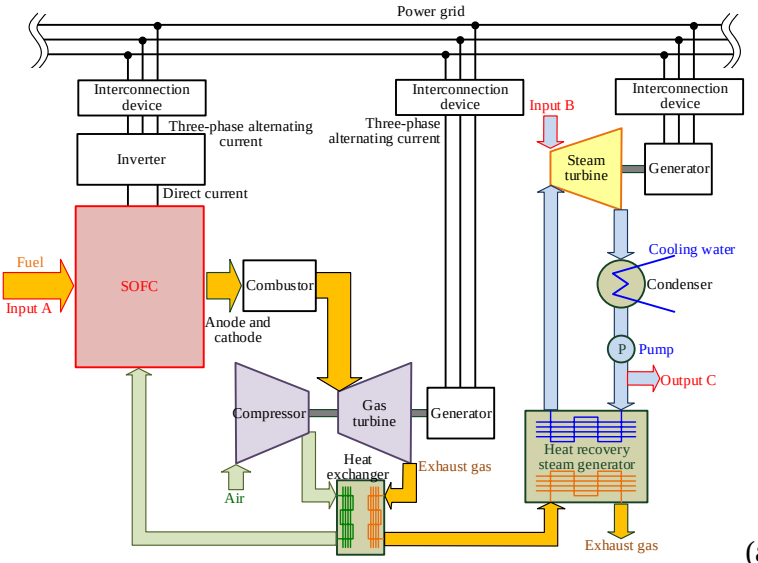
Power grid
Interconnection device
Interconnection device
Interconnection device
Three-phase alternating current
Three-phase alternating current
Inverter
Direct current
Input B
Steam turbine
Generator
Fuel
Input A
SOFC
Combustor
Anode and cathode
Cooling water
Condenser
P
Pump
Output C
Compressor
Gas turbine
Generator
Heat exchanger
Exhaust gas
Air
Heat recovery steam generator
Exhaust gas

(a)

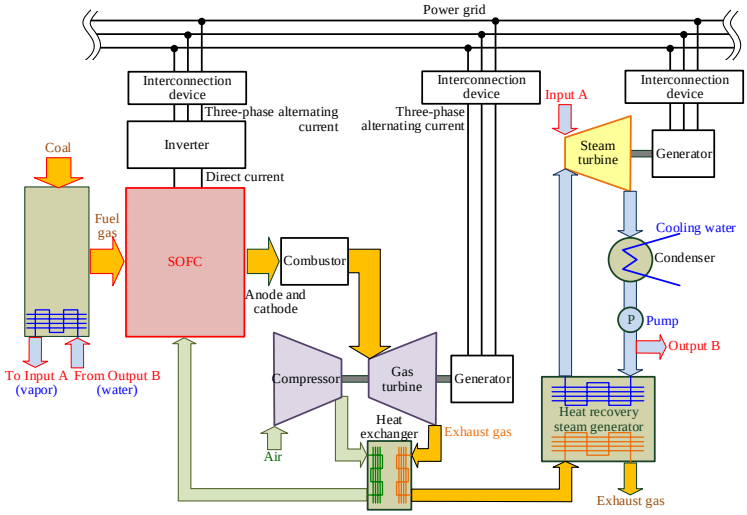
Power grid
Interconnection device
Interconnection device
Interconnection device
Three-phase alternating current
Three-phase alternating current
Inverter
Direct current
Input A
Steam turbine
Generator
Coal
Fuel gas
SOFC
Combustor
Anode and cathode
Cooling water
Condenser
P
Pump
Output B
To Input A (vapor)
From Output B (water)
Compressor
Gas turbine
Generator
Heat exchanger
Exhaust gas
Air
Heat recovery steam generator
Exhaust gas

(b)

Fig. 3

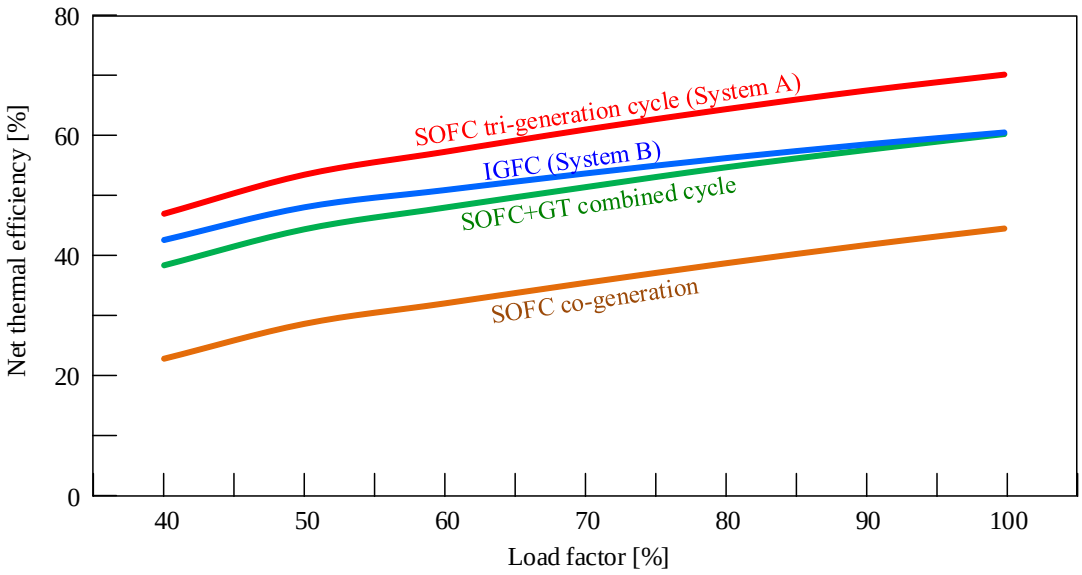
Net thermal efficiency [%]
Load factor [%]
SOFC tri-generation cycle (System A)
IGFC (System B)
SOFC+GT combined cycle
SOFC co-generation
0
20
40
60
80
40
50
60
70
80
90
100

Fig. 4

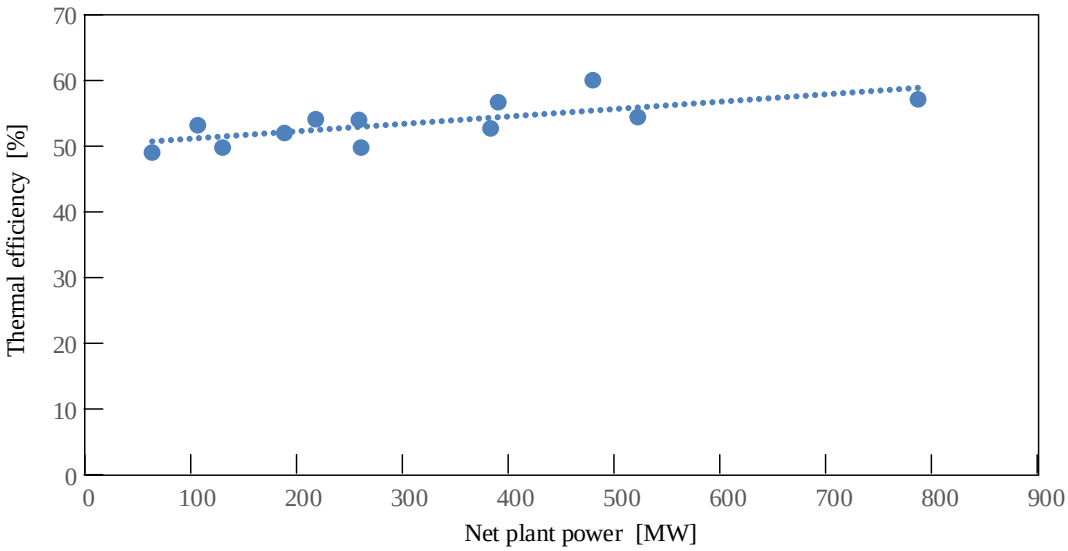
Thermal efficiency [%]
Net plant power [MW]
0
10
20
30
40
50
60
70
0
100
200
300
400
500
600
700
800
900

Fig. 5

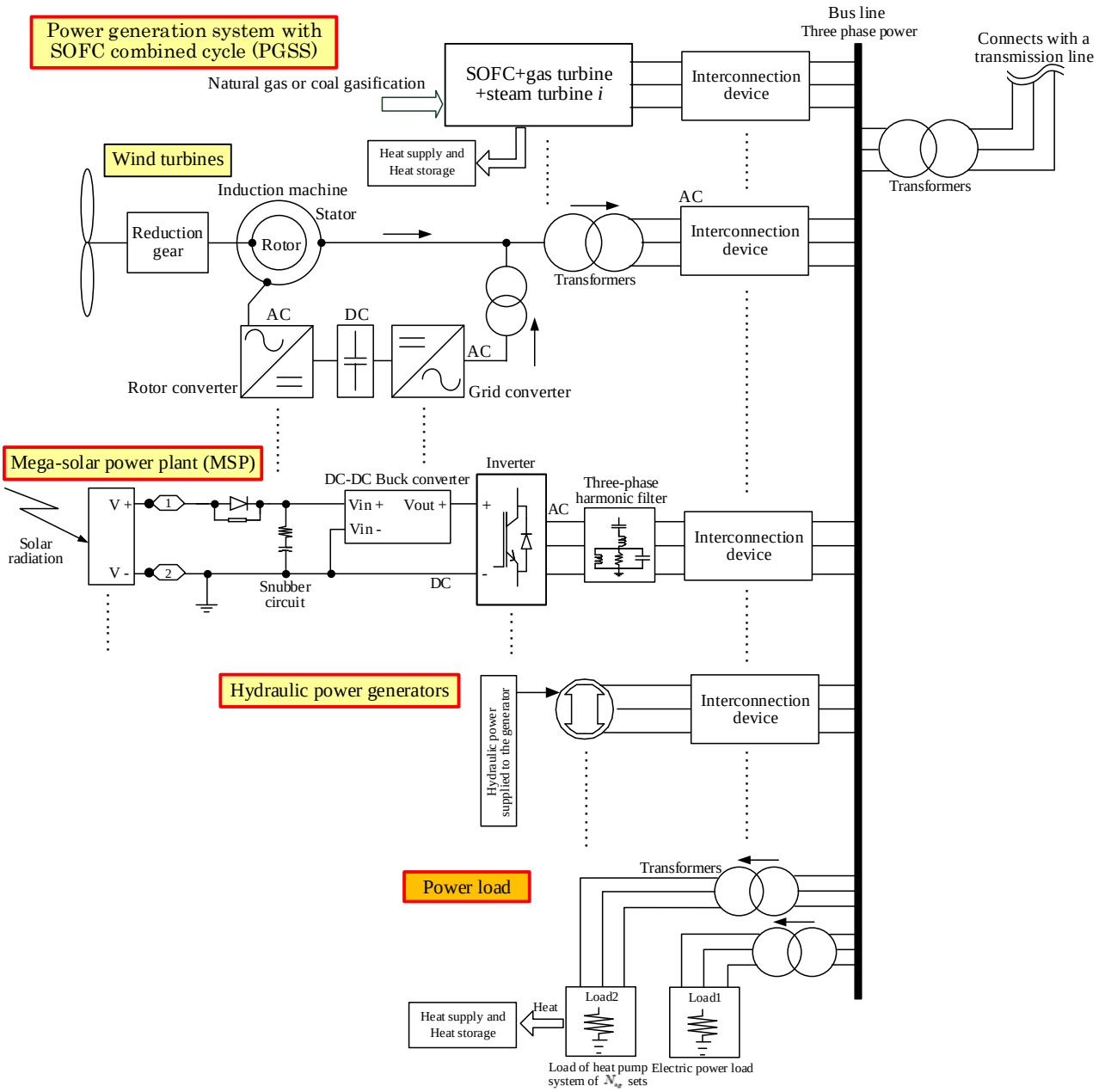
Power generation system with SOFC combined cycle (PGSS)
Natural gas or coal gasification
SOFC+gas turbine +steam turbine *i*
Heat supply and Heat storage
Interconnection device
Bus line
Three phase power
Connects with a transmission line
Transformers
Wind turbines
Induction machine
Stator
Rotor
Reduction gear
AC
Interconnection device
Transformers
AC
DC
AC
Rotor converter
Grid converter
Mega-solar power plant (MSP)
Inverter
DC-DC Buck converter
Three-phase harmonic filter
Solar radiation
V +
V -
1
2
Vin +
Vout +
Vin -
Snubber circuit
DC
AC
Interconnection device
Hydraulic power generators
Hydraulic power supplied to the generator
Interconnection device
Power load
Transformers
Load2
Load1
Heat
Heat supply and Heat storage
Load of heat pump system of N_{hp} sets
Electric power load

Fig. 6

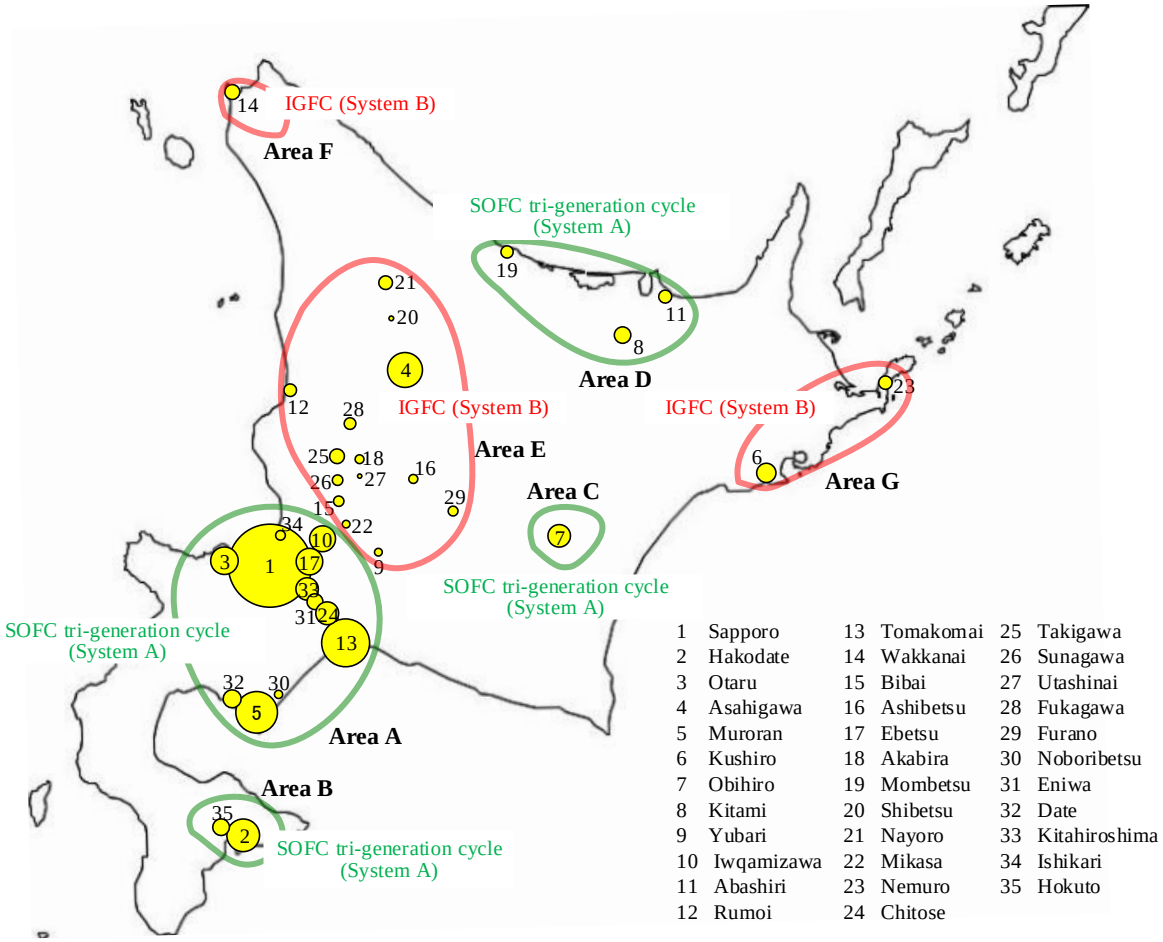
14
IGFC (System B)
Area F
SOFC tri-generation cycle
(System A)
19
21
20
11
8
4
Area D
12
28
IGFC (System B)
IGFC (System B)
23
Area E
25
18
16
6
26
27
Area G
15
29
Area C
34
22
10
7
3
1
17
9
SOFC tri-generation cycle
(System A)
33
31
24
SOFC tri-generation cycle
(System A)
13
32
30
5
Area A
Area B
35
2
SOFC tri-generation cycle
(System A)
1 Sapporo
2 Hakodate
3 Otaru
4 Asahigawa
5 Muroran
6 Kushiro
7 Obihiro
8 Kitami
9 Yubari
10 Iwqamizawa
11 Abashiri
12 Rumoi
13 Tomakomai
14 Wakkanai
15 Bibai
16 Ashibetsu
17 Ebetsu
18 Akabira
19 Mombetsu
20 Shibetsu
21 Nayoro
22 Mikasa
23 Nemuro
24 Chitose
25 Takigawa
26 Sunagawa
27 Utashinai
28 Fukagawa
29 Furano
30 Noboribetsu
31 Eniwa
32 Date
33 Kitahiroshima
34 Ishikari
35 Hokuto

Fig. 7

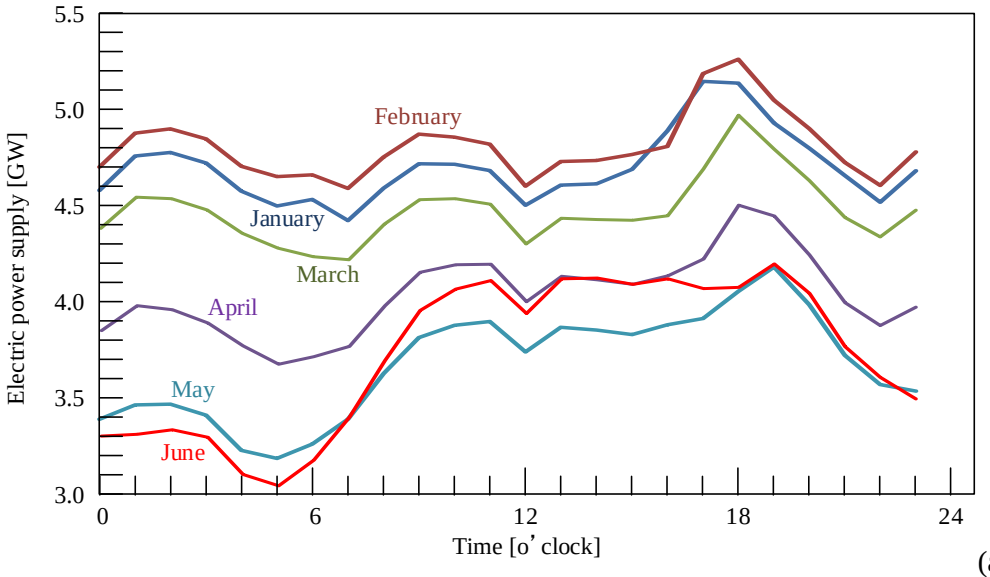
5.5
5.0
4.5
4.0
3.5
3.0
Electric power supply [GW]
February
January
March
April
May
June
0
6
12
18
24
Time [o' clock]

(a)

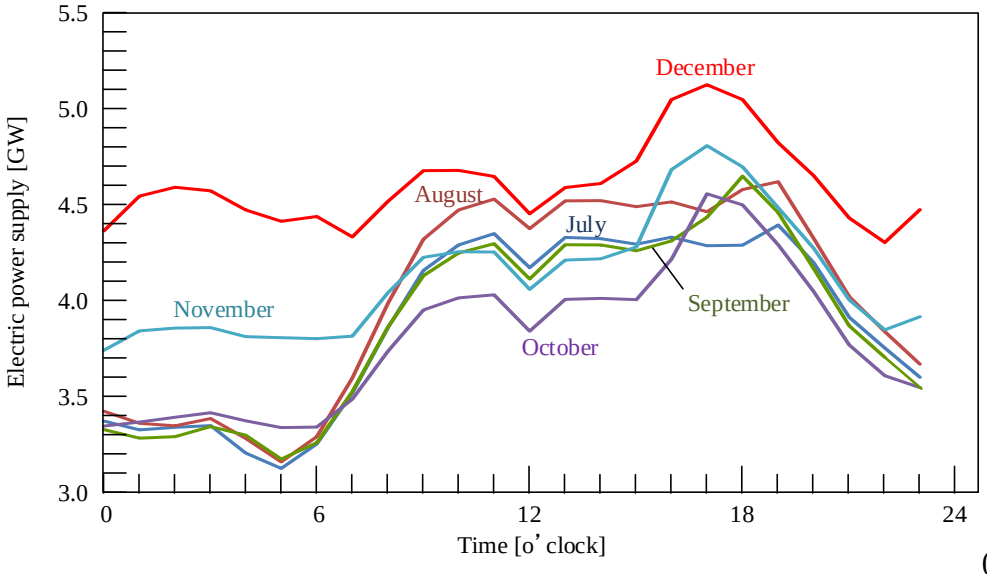
5.5
5.0
4.5
4.0
3.5
3.0
Electric power supply [GW]
December
August
July
September
November
October
0
6
12
18
24
Time [o' clock]

(b)

Fig. 8

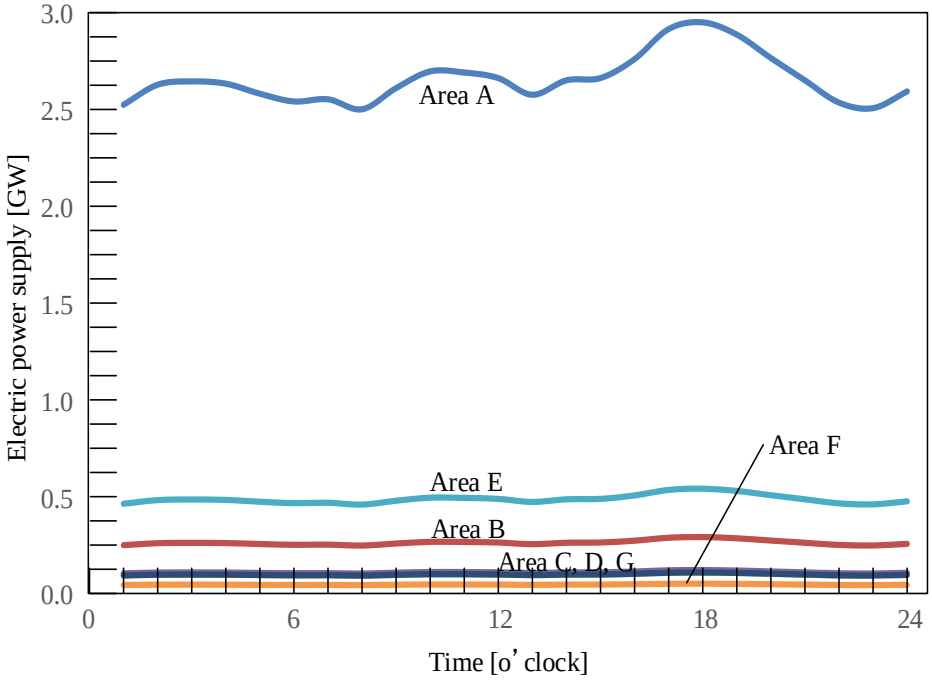

450

451 Fig. 9

452

453

454

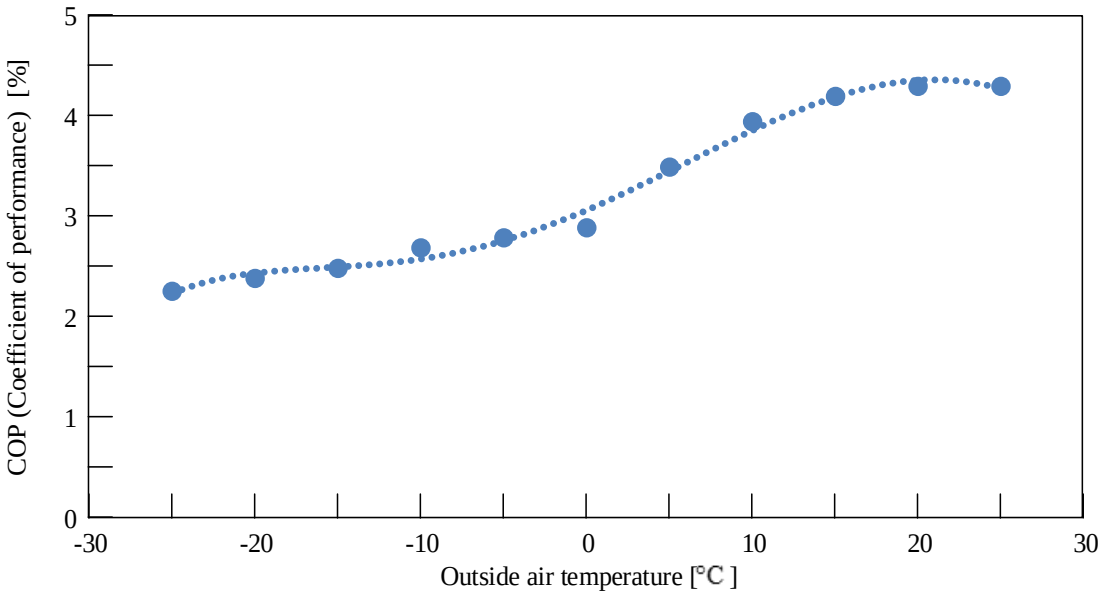

455

456 Fig. 10

457

458

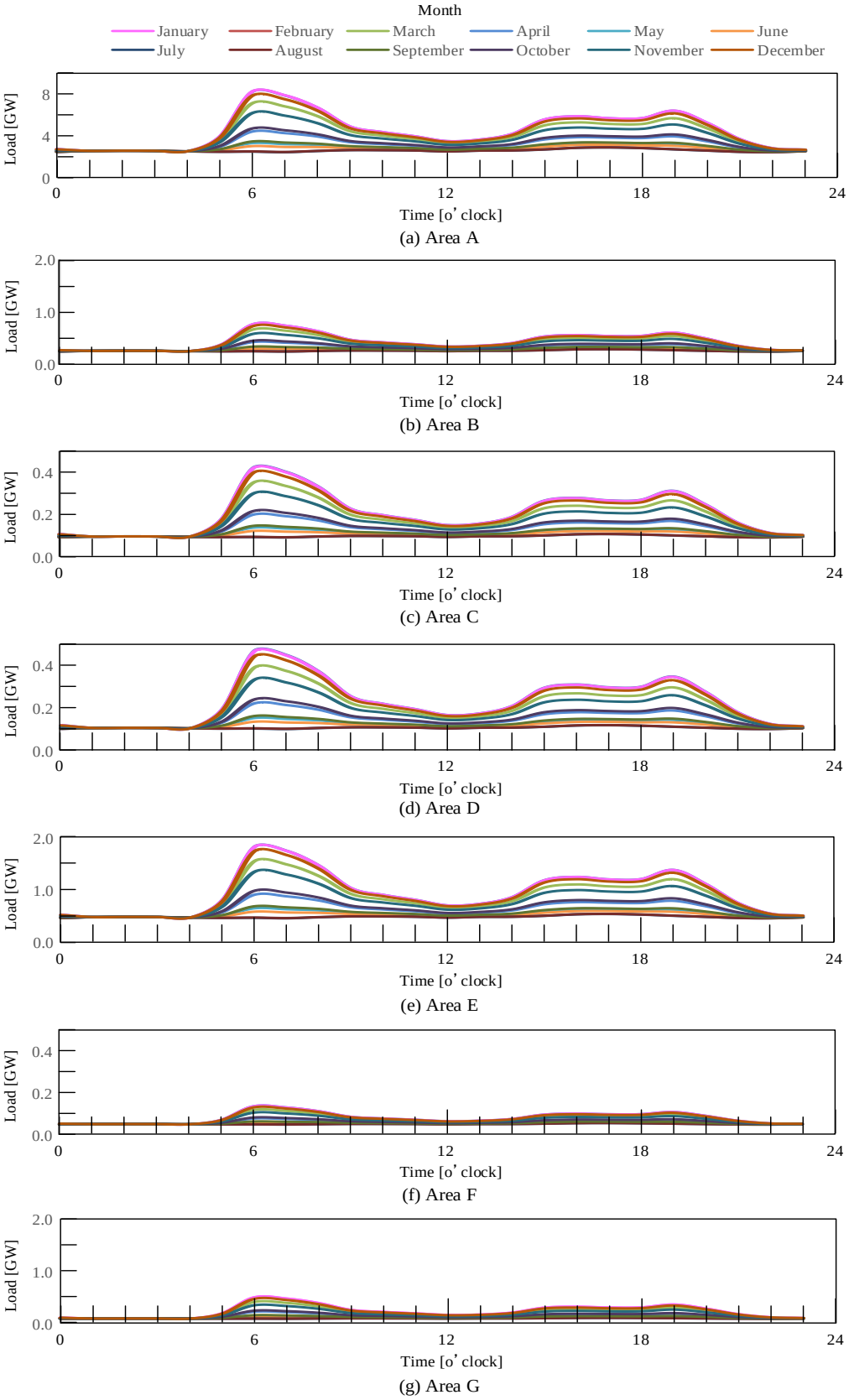

459

460 Fig. 11

461

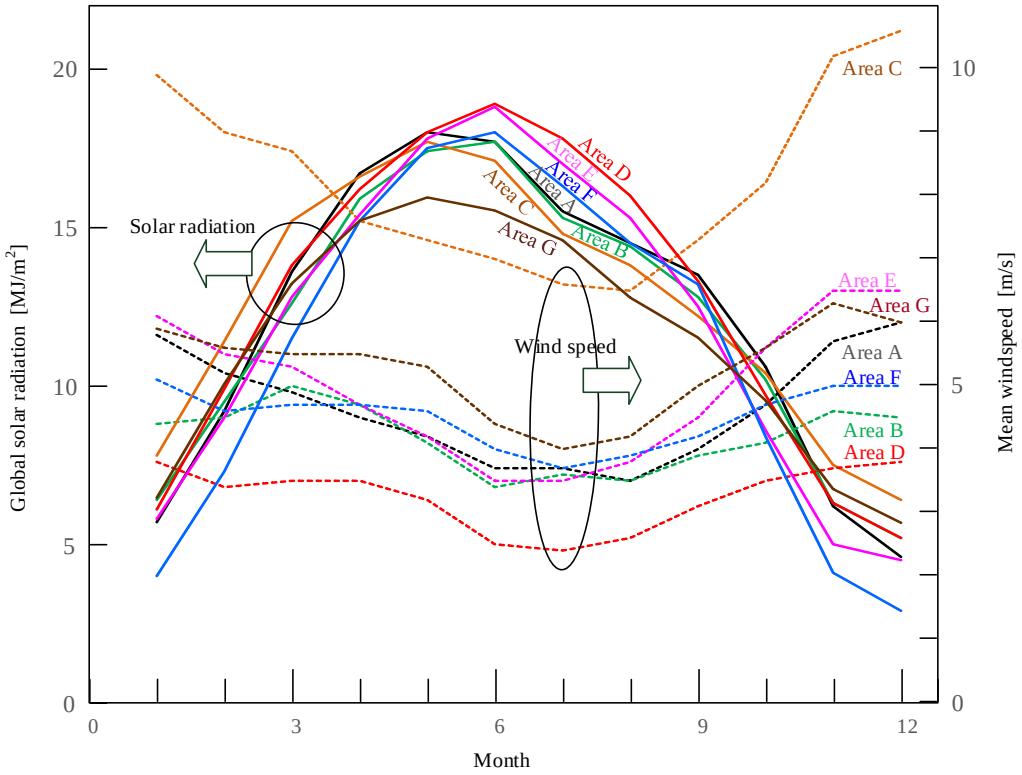
Global solar radiation [MJ/m2]
Mean windspeed [m/s]
Month
Solar radiation
Wind speed
Area C
Area D
Area E
Area F
Area A
Area B
Area G
Area C
Area E
Area G
Area A
Area F
Area B
Area D
0
3
6
9
12
0
5
10
15
20
0
5
10

Fig. 12

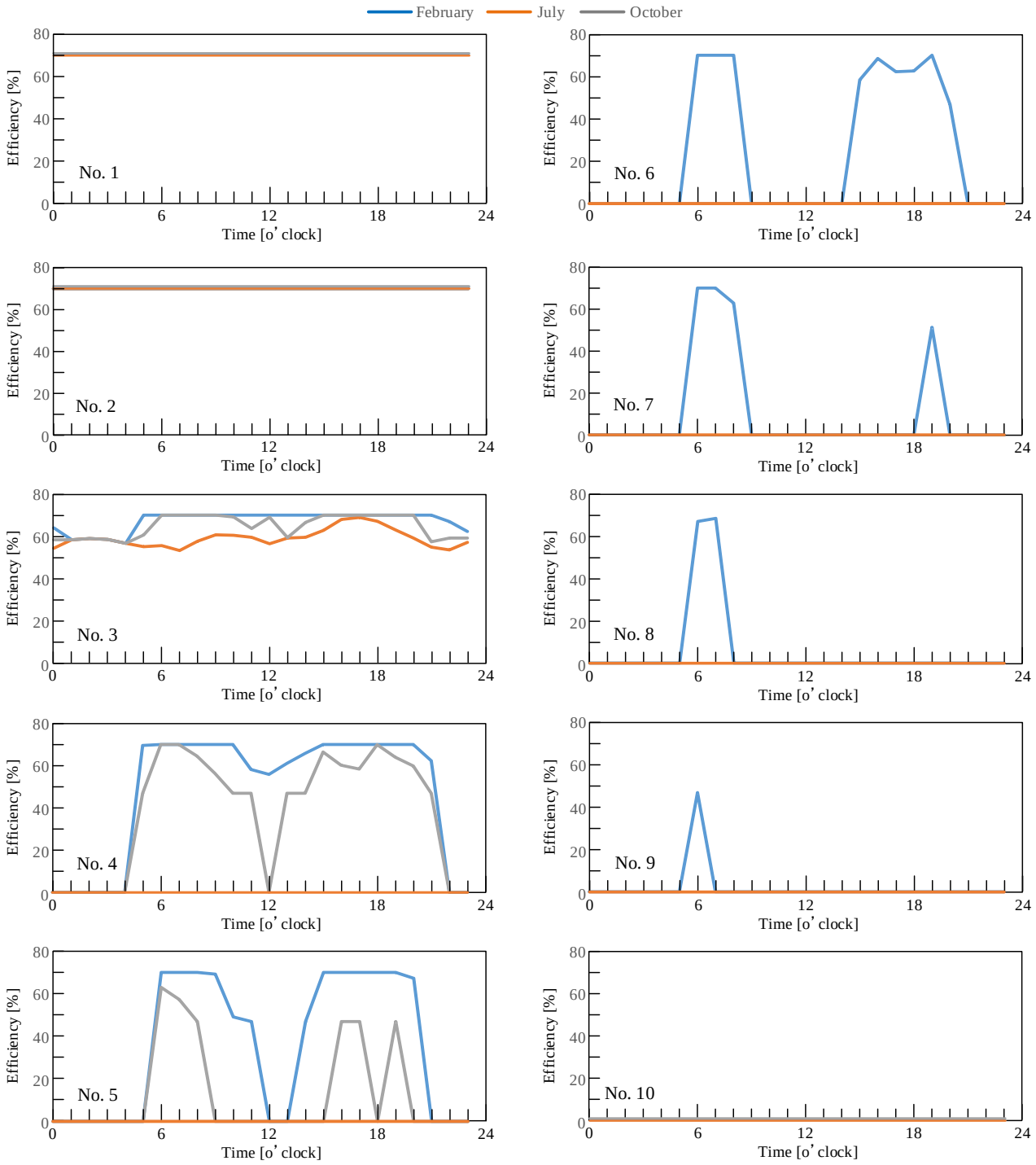
February
July
October
Efficiency [%]
Time [o' clock]
No. 1
No. 2
No. 3
No. 4
No. 5
No. 6
No. 7
No. 8
No. 9
No. 10

Fig. 13 (a)

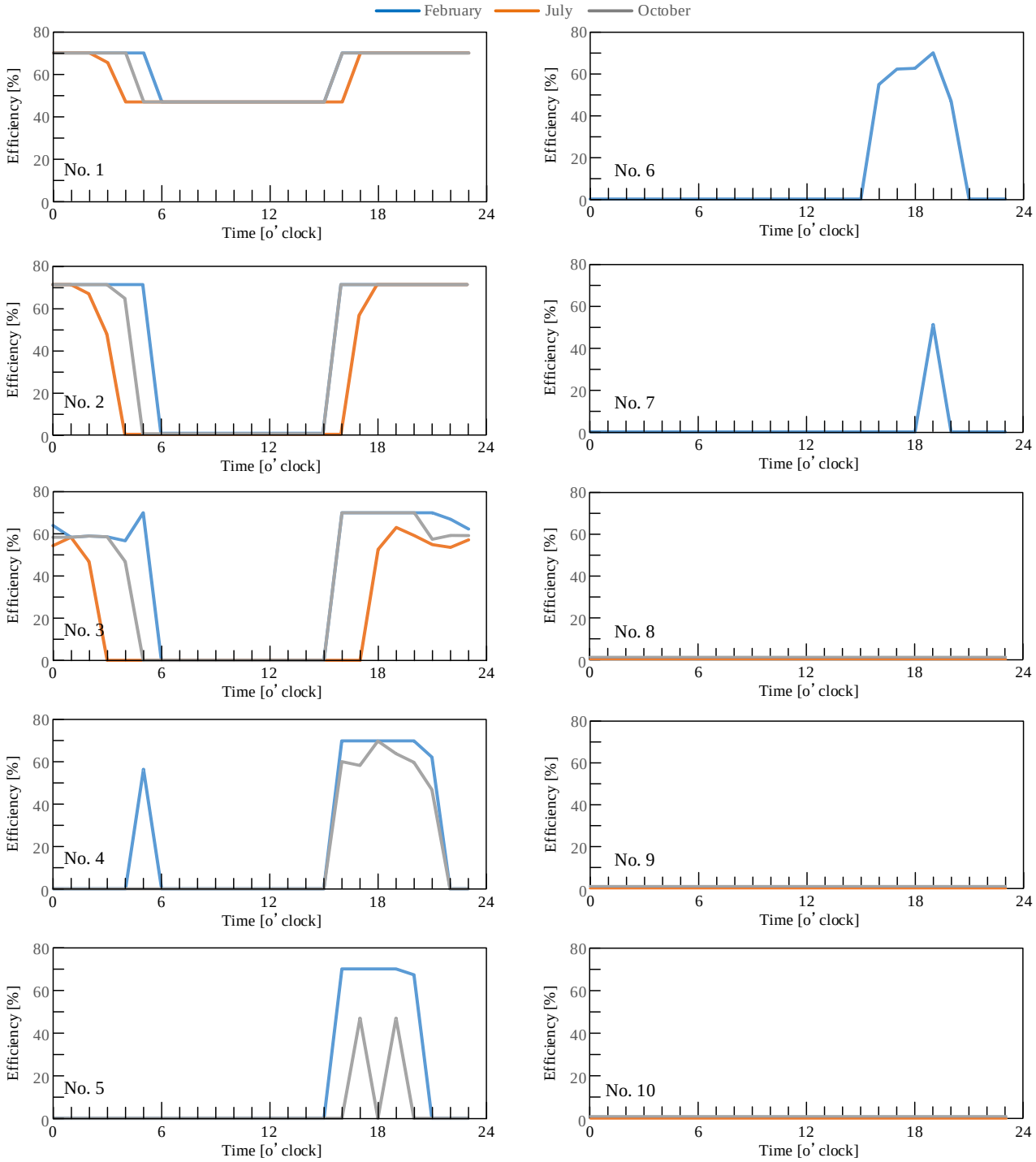
February
July
October
Efficiency [%]
Time [o' clock]
No. 1
No. 2
No. 3
No. 4
No. 5
No. 6
No. 7
No. 8
No. 9
No. 10

Fig. 13 (b)

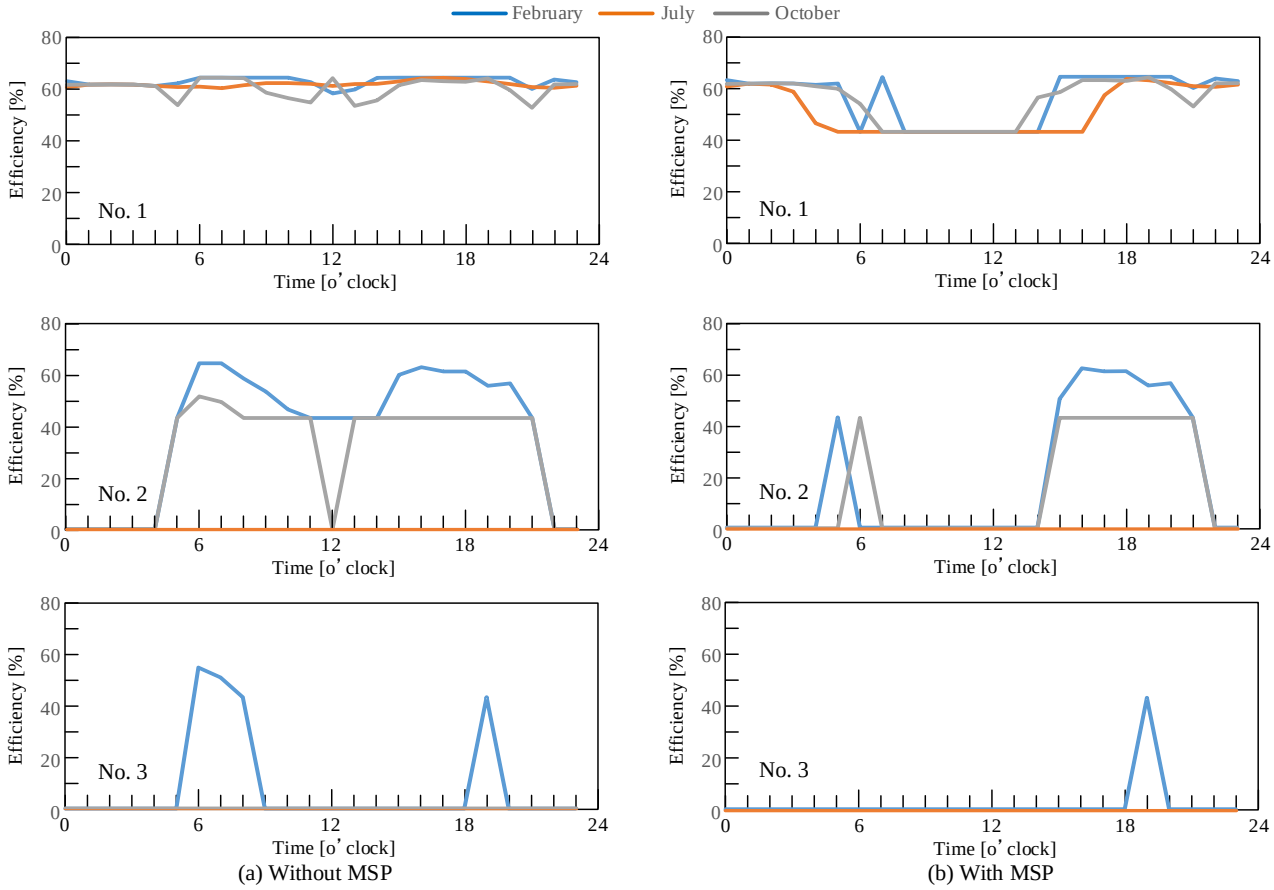

(a) Without MSP (b) With MSP

474

475 Fig. 14

476

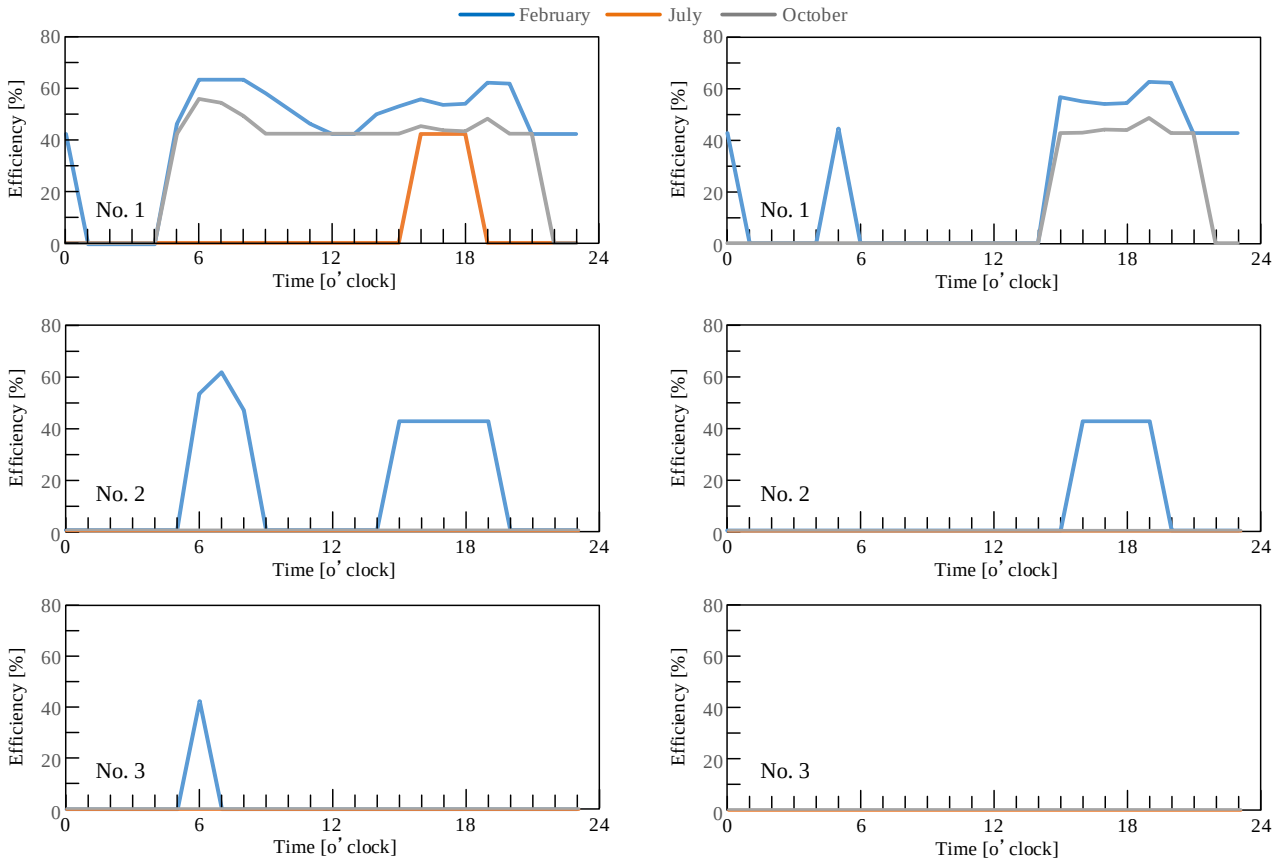

(a) Without MSP (b) With MSP

477

478 Fig. 15

479

480

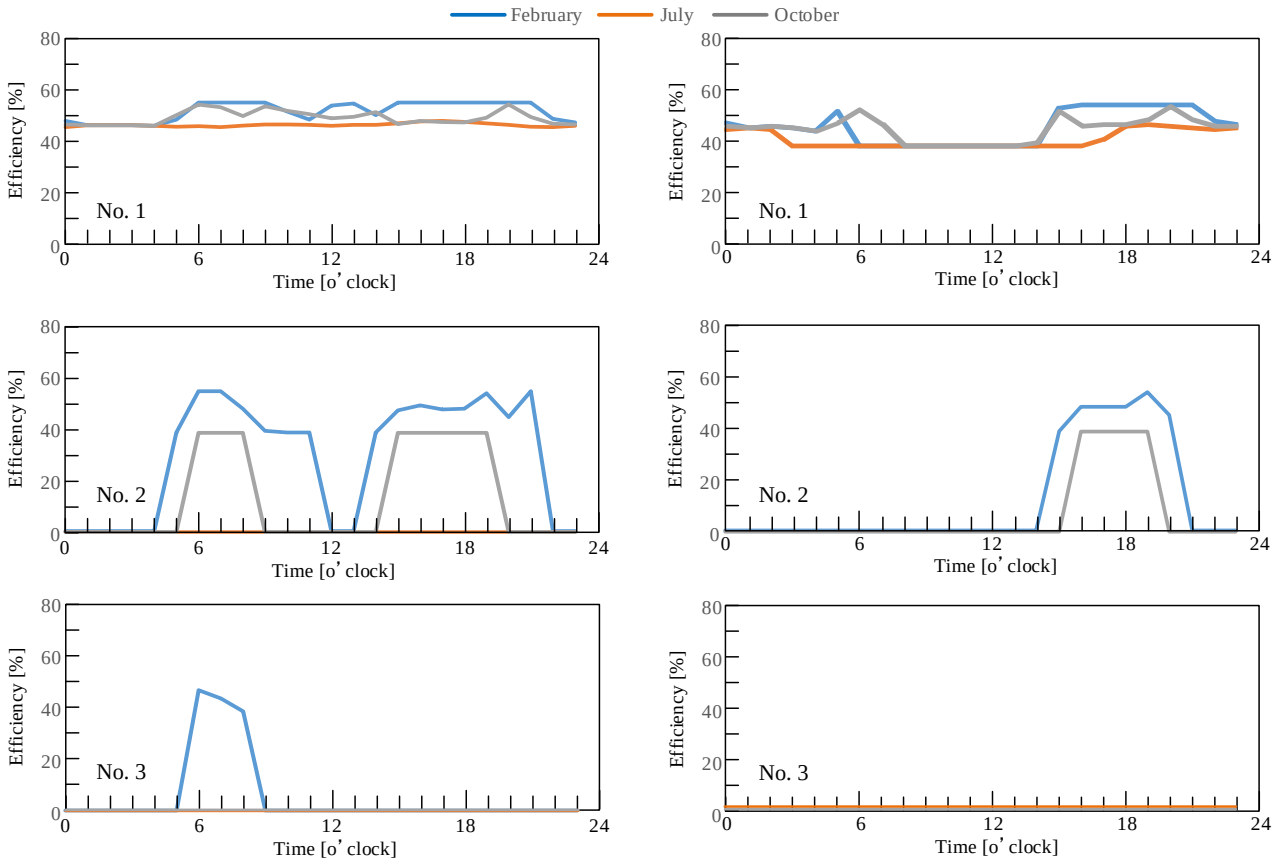

(a) Without MSP

(b) With MSP

Fig. 16

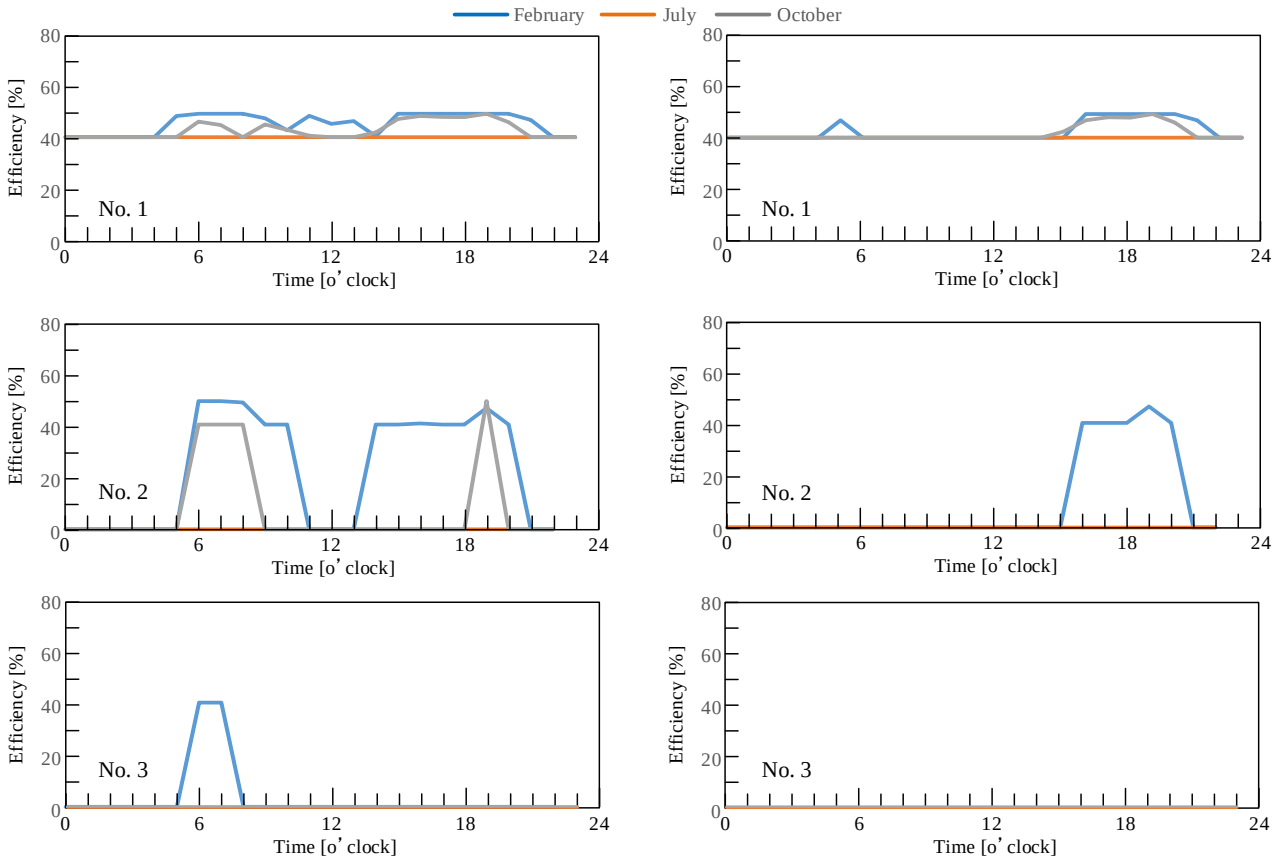

(a) Without MSP (b) With MSP

485

486 Fig. 17

487

488

489

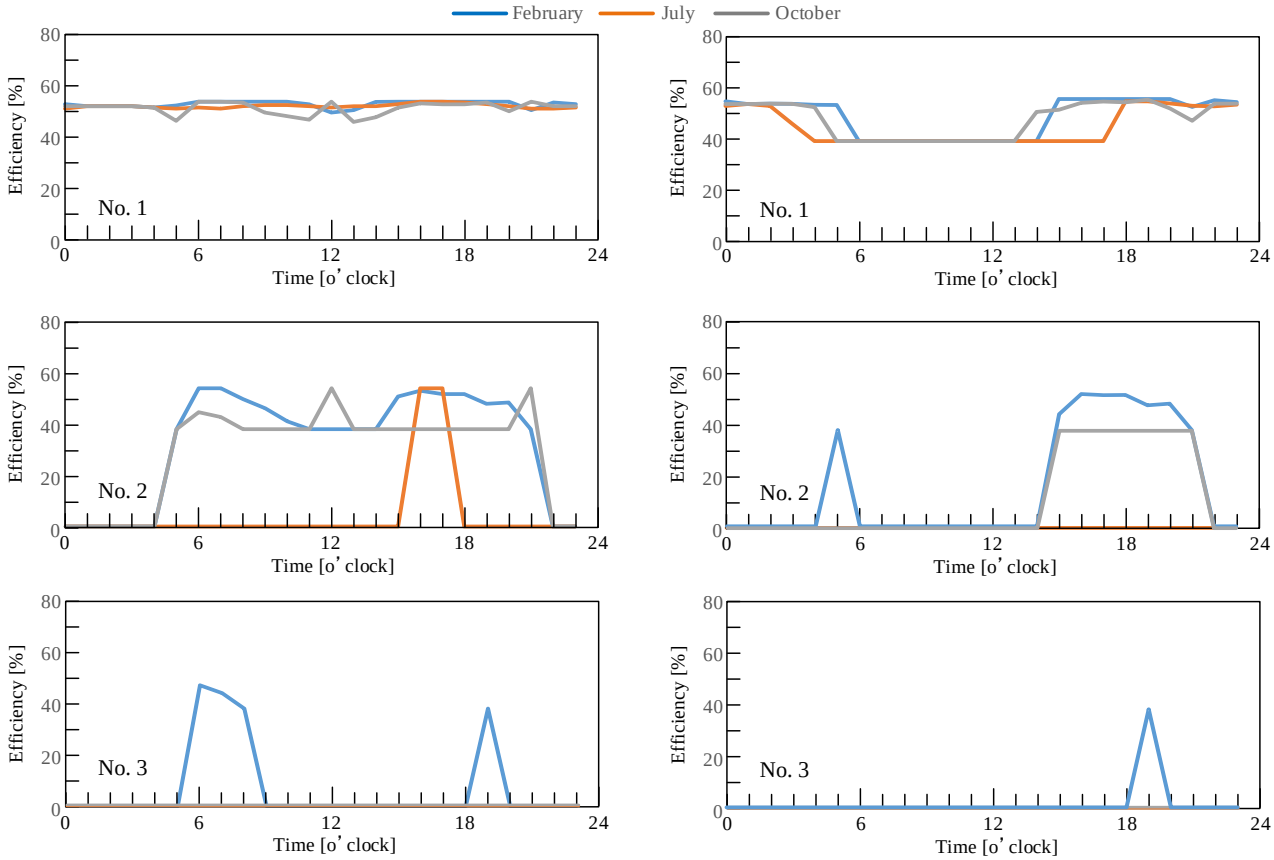

(a) Without MSP (b) With MSP

Fig. 18

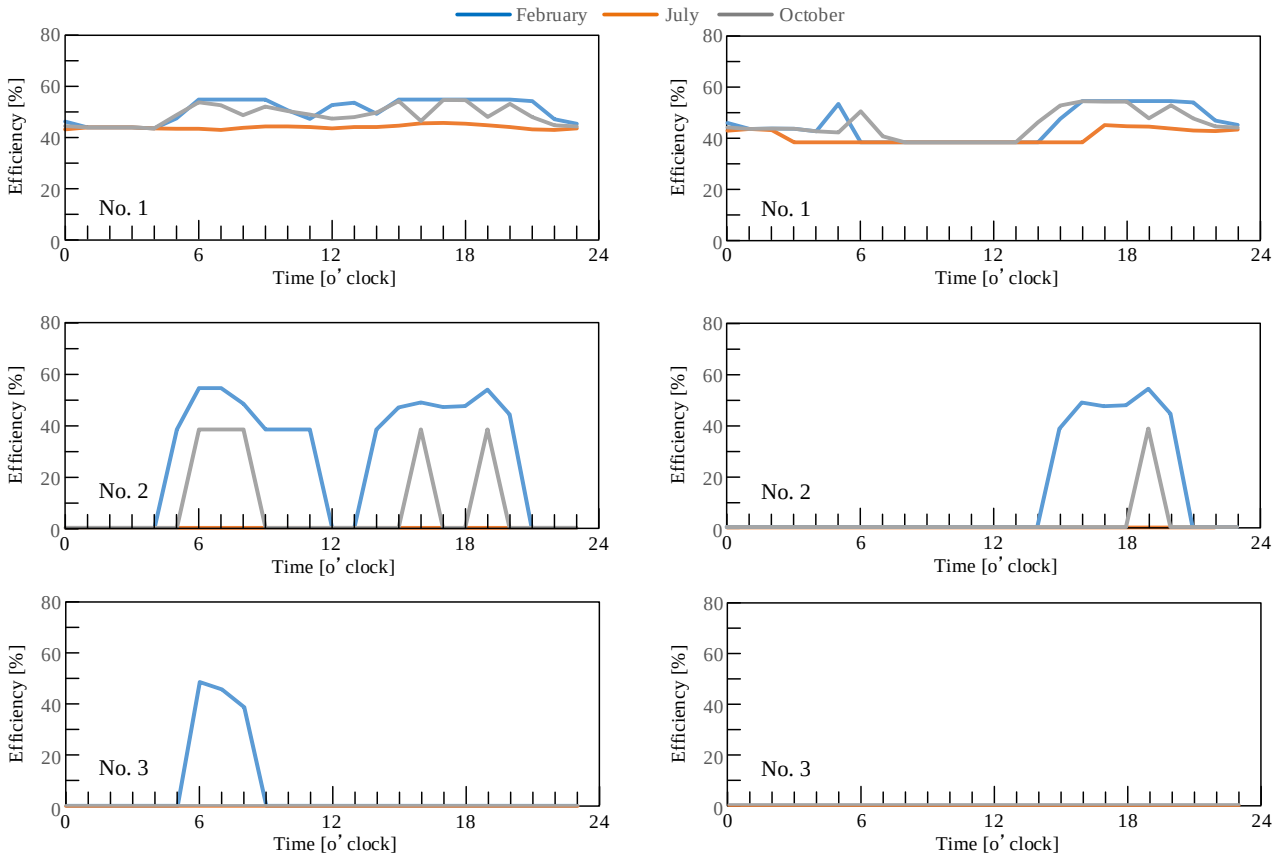

(a) Without MSP

(b) With MSP

Fig. 19

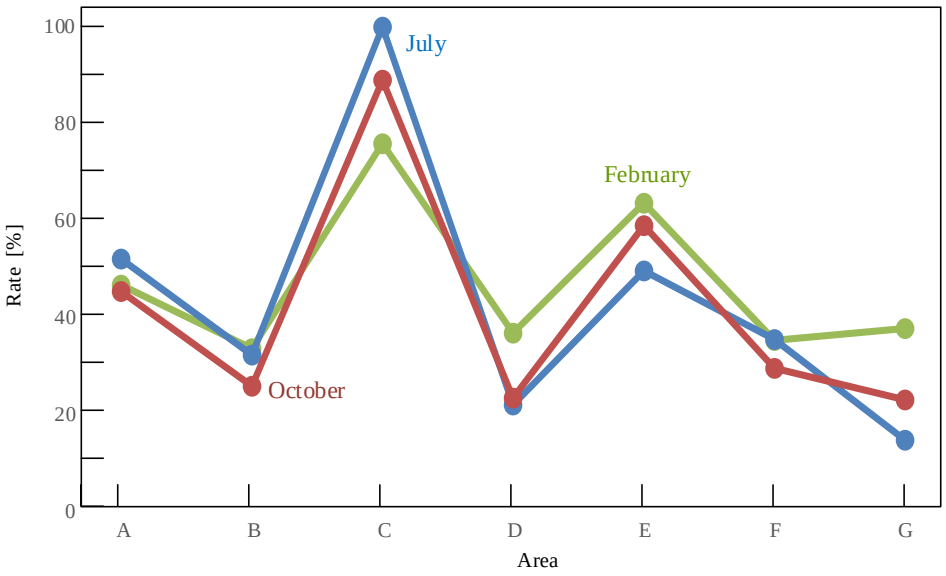

498

499 Fig. 20

500

501

502

503

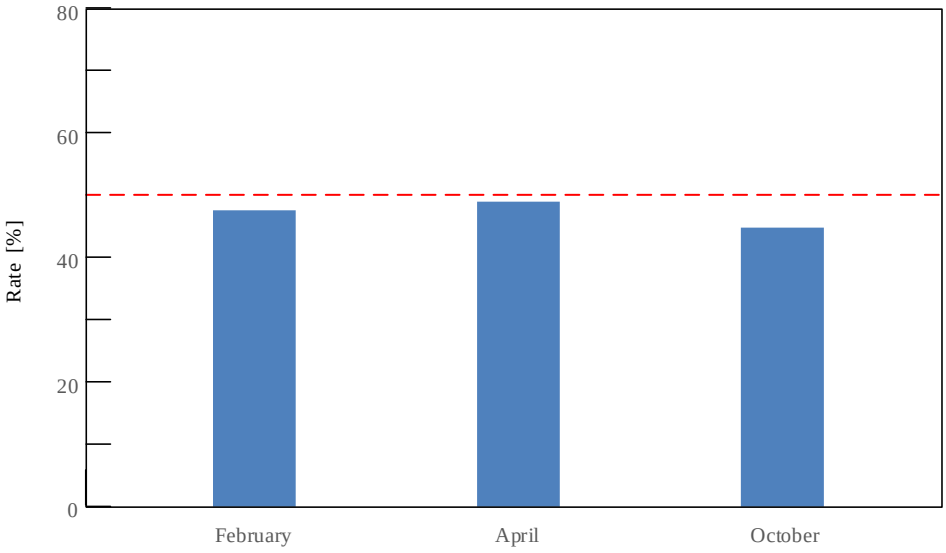

504

505 Fig. 21

506

507

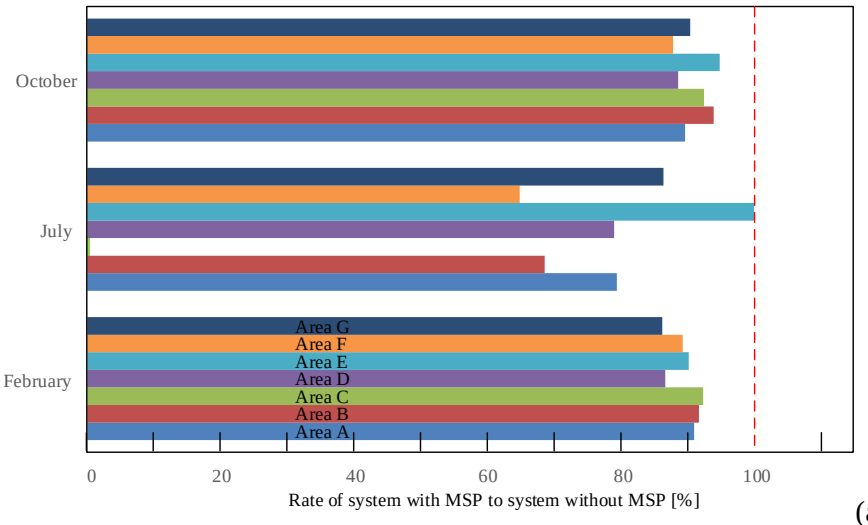

508 (a)

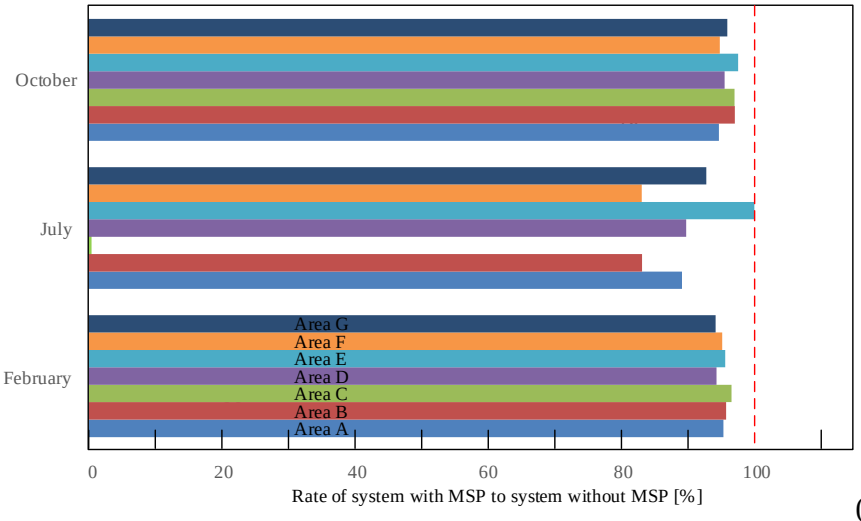

509 (b)

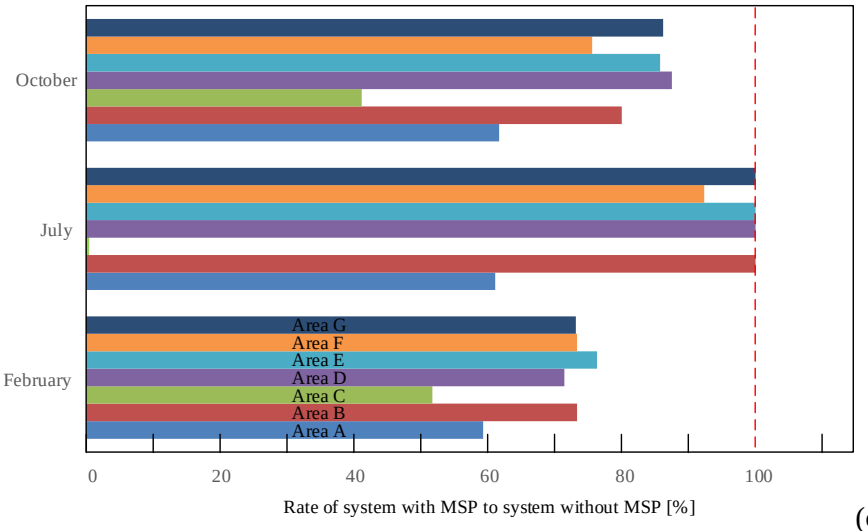

510 (c)

511 Fig. 22

512

Table 1. Number of PGSSs installed

Area	Maximum power load [GW]	Capacity [GW]	Installed number	Area of MSP [km^2]	Location of MSP	Hydro power [GW]
Area A	8.29	1.0	10	1000	Muroran	
Area B	0.771	0.290	3	12.5	Hakodate	
Area C	0.420	0.157	3	16.0	Obihiro	0.1
Area D	0.472	0.180	3	21.0	Abashiri	
Area E	1.822	0.640	3	140	Asahigawa	0.2
Area F	0.128	0.048	3	5.0	Wakkanai	
Area G	0.496	0.184	3	8.0	Kushiro	

Table 2. Net thermal efficiency of areas A–G

	Without mega-solar power plant				With mega-solar power plant			
Area	February [%]	July [%]	October [%]	Average [%]	February [%]	July [%]	October [%]	Average [%]
Area A	67.6	66.5	65.4	**66.5**	64.5	59.2	61.9	**61.9**
Area B	58.1	62.0	54.0	**58.0**	55.6	51.6	52.4	**53.2**
Area C	50.3	42.5	45.1	**46.0**	48.5	No operation	43.8	**46.2**
Area D	49.2	46.2	46.4	**47.3**	46.4	41.5	44.4	**44.1**
Area E	45.1	40.9	43.6	**43.2**	43.1	40.9	42.5	**42.2**
Area F	49.3	52.4	47.0	**49.6**	46.9	43.6	44.5	**45.0**
Area G	48.7	44.1	47.0	**46.6**	45.8	40.9	45.1	**44.0**